In situ Validation of the Source of Thin Layers Detected by NOAA Airborne Fish Lidar

Dr. James H. Churnside
NOAA Earth System Research Laboratory, CSD3
325 Broadway
Boulder, CO 80305
phone: (303) 497-6744 fax: (303)497-5318 email: james.h.churnside@noaa.gov

Award Number: N0001410IP20035 & N0001409IP20039
http://www.esrl.noaa.gov/csd/groups/csd3/instruments/floe/

LONG-TERM GOALS

Our long-term goal is to understand how physical-biological, biological-biological and chemical-biological interactions control the formation, maintenance and dissipation of thin layers of plankton and how the resulting thin layers impact *in situ* and remote sensing technologies of critical interest to the Navy. We are also interested in improving our ability not only to detect, characterize and map the temporal and spatial extent of thin layers, but also to improve our ability to predict their occurrence in a variety of ocean environments.

OBJECTIVES

Our short-term objective is to evaluate the relative importance of large non-spheroid phytoplankton and zooplankton in generating the thin optical backscattering layers detected by the NOAA airborne fish lidar in a variety of coastal and oceanic environments. The existing system clearly has the capability of detecting thin layers and mapping their coherence and spatial extent in a wide variety of coastal and oceanic environments.

APPROACH

The approach was to use a series of field experiments to evaluate the source of the thin layers of high backscattering detected by airborne fish lidar. We are particularly interested in determining the degree to which the cross polarization detector system (and other characteristics) of the airborne fish lidar make it sensitive to thin layers of large, non-spheroid phytoplankton and/or zooplankton, or other types of layered particulate material that are common in coastal waters. In designing these field experiments, we have tried to minimize costs while maximizing the chances of *in situ* verification/validation of the sources of thin layers that can be detected by the NOAA fish lidar. Given this, we designed a series of field experiments where we deploy the fish lidar from a small plane and use real-time analysis of lidar data to identify areas with thin backscattering layers that Dr. Donaghay and coworkers from the University of Rhode Island would sample with a small boat equipped with the *in situ* optical sensors and discrete sampling systems needed to verify and optically characterize the source of the observed lidar signals. Real-time analysis of the lidar data was facilitated by transmitting the lidar data to the

Report Documentation Page

Form Approved
OMB No. 0704-0188

1. REPORT DATE	2. REPORT TYPE	3. DATES COVERED
30 SEP 2011		**00-00-2011 to 00-00-2011**

4. TITLE AND SUBTITLE	5a. CONTRACT NUMBER
In situ Validation of the Source of Thin Layers Detected by NOAA Airborne Fish Lidar	5b. GRANT NUMBER
	5c. PROGRAM ELEMENT NUMBER
6. AUTHOR(S)	5d. PROJECT NUMBER
	5e. TASK NUMBER
	5f. WORK UNIT NUMBER
7. PERFORMING ORGANIZATION NAME(S) AND ADDRESS(ES) **NOAA Earth System Research Laboratory, CSD3,325 Broadway,Boulder,CO,80305**	8. PERFORMING ORGANIZATION REPORT NUMBER
9. SPONSORING/MONITORING AGENCY NAME(S) AND ADDRESS(ES)	10. SPONSOR/MONITOR'S ACRONYM(S)
	11. SPONSOR/MONITOR'S REPORT NUMBER(S)

12. DISTRIBUTION/AVAILABILITY STATEMENT
Approved for public release; distribution unlimited

13. SUPPLEMENTARY NOTES

14. ABSTRACT

15. SUBJECT TERMS

16. SECURITY CLASSIFICATION OF:			17. LIMITATION OF ABSTRACT	18. NUMBER OF PAGES	19a. NAME OF RESPONSIBLE PERSON
a. REPORT **unclassified**	b. ABSTRACT **unclassified**	c. THIS PAGE **unclassified**	**Same as Report (SAR)**	**8**	

surface in real time so that all of the information that would be available to an airborne operator is available to the scientists on the boat.

At each station the URI group used their ship-deployed slow-descent high-resolution profiler to collect replicate profiles of fine-scale vertical structure of (a) spectral absorption and attenuation by dissolved plus particulate material, (b) spectral absorption colored dissolved organic material, (c) optical backscatter, (d) chlorophyll a fluorescence, (e) fluorescence of colored dissolved organic matter, (f) temperature, salinity, and density, and (g) oxygen. The resulting data were used to calculate the vertical fine-scale structure of particulate absorption and scattering and a series of derived parameters.. Although most of these profiles were collected in locations where layers were detected by the lidar, we collected some in areas where no lidar layers were detected. The URI group used these *in situ* optical profiles to guide the collection of discrete samples from features of interest for immediate analysis of phytoplankton composition using video microscopy and analysis of individual particle optical characteristics using our CytoSense scanning-in-line flow cytometer. Samples were also preserved for analysis in the lab of phytoplankton composition and abundance. Samples for analysis of zooplankton size, abundance and composition were collected from features of interest using a pump and as integrated samples using a vertical net tow. In addition, several other groups, not supported by ONR, brought additional instrumentation, deployed from additional platforms. These include several holographic cameras from Johns Hopkins University and WET Labs, profiling gliders from the Naval Research Laboratory, and a polarization-sensitive volume scattering instrument from Sequoia Scientific.

The choice of a May campaign in the East Sound was made for several reasons. First, past work in this area gave Donaghay, Sullivan and Rines considerable confidence that we could not only expect the periodic occurrence of intense thin layers of phytoplankton and zooplankton, but that we could also sample these layers from small boats for low cost and operated in a highly flexible manner. Second, Churnside has experience working with a retired NOAA pilot in the area who has a small aircraft suitable for flying the lidar system. Equally importantly, the pilot is flexible and interested in the proposed effort and willing to participate at a very reasonable cost. This combination of past experience in the area as well as low cost and flexibility of both airborne and ship operations produced two spectacular data sets while minimizing costs, despite the high lidar attenuation typical of inland waters.

WORK COMPLETED

Lidar data from the 2009 experiment have been compared with in-water measurements at 532 nm using a lidar model based on the quasi-single-scattering approximation (Churnside, 2008). The model used the in-water estimates of diffuse-attenuation coefficient and the volume scattering function for unpolarized light at a scattering angle of 150˚ to estimate the co-polarized lidar return. Sampling showed that the scattering particles in 2009 were a single species of diatom, so we attempted to calculate the scattering matrix for polarized light for this species. Because of the extreme ellipticity of this species (50 to 1), we were unable to obtain satisfactory theoretical results.

The second field experiment was completed, with 27 flights over a period of 14 days. A morning and an afternoon flight was made each day but one. The locations of interesting layers were communicated to the three surface vessels (one operated by the University of Rhode Island group supported by this program, one operated by the Naval Research Laboratory under separate funding, and one operated by WET Labs with their own funding) in real time.

These data were divided into 299 transects along the length of the sound. For each transect, we produced an echogram of the lidar return and a plot of the depth and strength of the maximum return for each profile. These were also compared with in-water measurements using an improved mathematical model.

RESULTS

A typical comparison of measured and calculated lidar profiles from the 2009 data is presented in Figure 1. The theoretical curve starts at the minimum measurement depth of 1 m, and the attenuation at 1 m was assumed for the first meter of propagation. For this curve, the measurements were averaged into 11 cm depth bins to match the sampling resolution of the lidar. The measured profiles include a return from atmospheric aerosols above the surface, a specular surface reflection in two of the five co-polarized returns, and the subsurface return. The lidar data are sampled with an 11 cm depth resolution, but the returns are averaged over a little more than a meter in depth by the finite pulse length of the laser and by the tilt of beam. The attenuation of the co-polarized return is well approximated by the diffuse-attenuation coefficient for unpolarized light. The peak return from the layer is overestimated by the theory, which does not consider the averaging by the finite pulse length. Note that the theoretical curve generally overestimates the lidar return. This was common, and we are looking into the reasons for the bias. Another typical feature that shows up in Figure 1 is that the increase in signal at the layer is greater relative to the return above for the cross-polarized return than for the co-polarized return. The depth of the layer (starting at about 5 m) in the lidar returns corresponds to a density jump and an increase in chlorophyll concentration. A larger increase in chlorophyll concentration at about 10 m does not show up in either the measured lidar returns or the return calculated from the optical parameters measured on the same casts. The volume scattering coefficient shows the expected increase at 5 m, but does not show the same large increase at 10 m as does the chlorophyll.

Because of the absolute difference between the measured and theoretical curves in Figure 1, we performed a careful analysis of the lidar calibration. We also improved the lidar model to include a surface reflection from small, steep wave facets and the depth averaging caused by the finite laser pulse length. An example is shown in Figure 2.

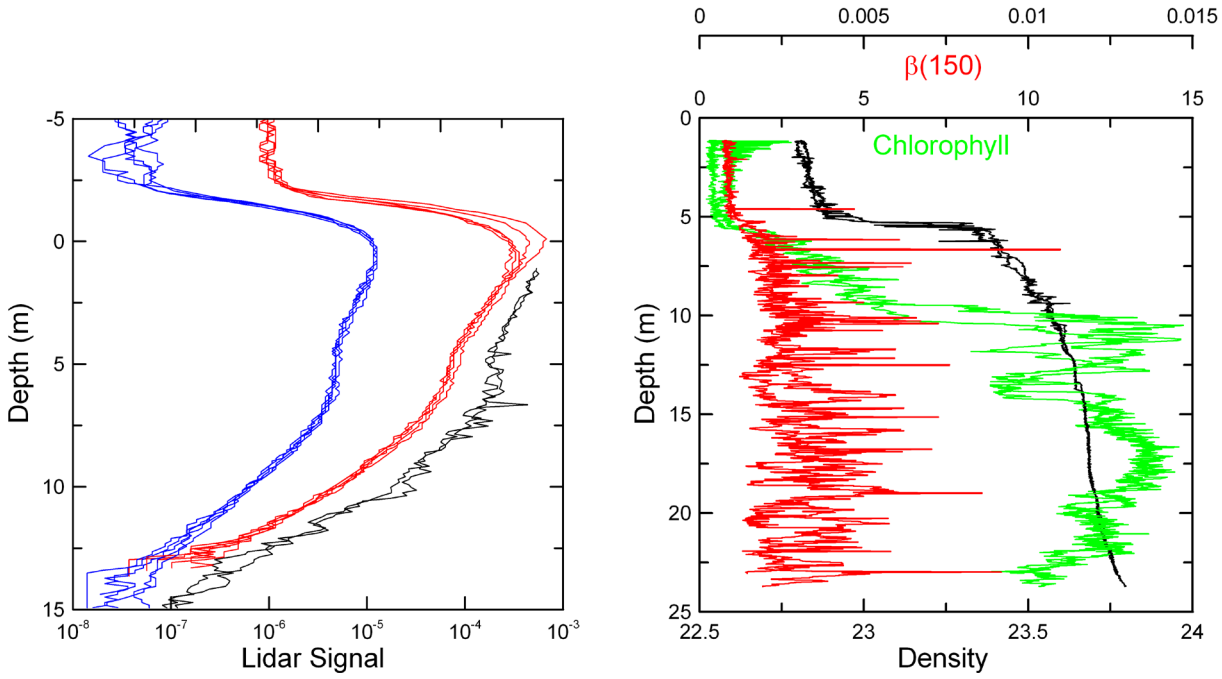

Fig. 1. The left panel is a typical lidar profile taken near a cast of the University of Rhode Island high resolution profiler. Blue lines are five consecutive cross-polarized lidar returns, red lines are five co-polarized lidar returns, and black lines is the theoretical curve from the in-water measurements made with two consecutive casts at the same location. The right panel is the density (black,) ac-9 chlorophyll concentration(green), and volume scattering coefficient at a scattering angle of 150˚ (red) from the two casts.

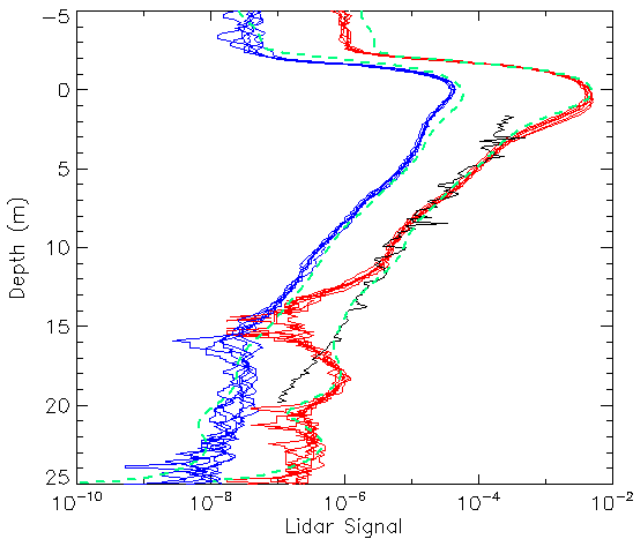

Fig. 2. Comparison of the modeled lidar return from a cast of the University of Rhode Island high resolution profiler and the measured lidar profile nearby. Blue lines are five consecutive cross-polarized lidar returns, red lines are five co-polarized lidar returns. The dashed green line shows the modeled lidar return from in situ data, taking into account the impulse response of the lidar system, surface reflections, and depolarization by scattering layers. The black line, shown for reference, is the simple theoretical model using diffuse attenuation and volume backscattering.

Figure 3 shows the lidar returns along a typical transect of 2010. At the bottom is a chart of the sound, rotated so that the long axis is horizontal. The specific flight track for this transect is plotted as a black line, which is roughly down the center of the sound. At the top is a lidar echogram with each profile normalized by its maximum value, and the other values color coded according to the color bar to the right. The horizontal axis is km from the head of the sound, and this is aligned with the chart. The two plots in the center are depth and cross-polarized volume scattering coefficient at the peak of the return, also aligned with the chart. This layer is associated with the pycnocline.

There are several interesting features in Figure 3. The layer generally gets deeper and thicker farther into the sound. At the same time, the peak scattering intensity is near the center, and has an almost periodic structure with a wavelength of about 1.5 km. While difficult to see in this figure, we point out that there is a small scale wave structure about 8 km from the head of the sound that has the characteristic of an internal-wave train with a wavelength of about 100 m.

One of the big questions has been whether or not it would be possible to discriminate between large phytoplankton and zooplankton in the lidar signatures. In 2009, there were virtually no zooplankton, and it was not possible to address this question. In 2010, there were regions of high zooplankton concentration, and there are differences in the lidar return. Figures 4 and 5 illustrate these differences. Figure 4 is a segment of a layer believed to be primarily phytoplankton. The appearance is similar to those observed in 2009, with relatively slow variations in backscattering intensity along the flight track. The power spectrum of the peak return of each profile as a function of horizontal spatial frequency shows a power-law with a slope of -5/3, which is characteristic of turbulence. Figure 4,

from a region where large numbers of zooplankton were reported, is qualitatively different, containing several very small, strong targets. This type of echogram was not seen in 2009. The power spectrum is not a turbulent spectrum, which suggests that the individual particles in this layer are not merely passively following a turbulent flow, but are either actively aggregating or being impacted by zooplankton grazing or some highly spatially variable mortality or growth controlling process.

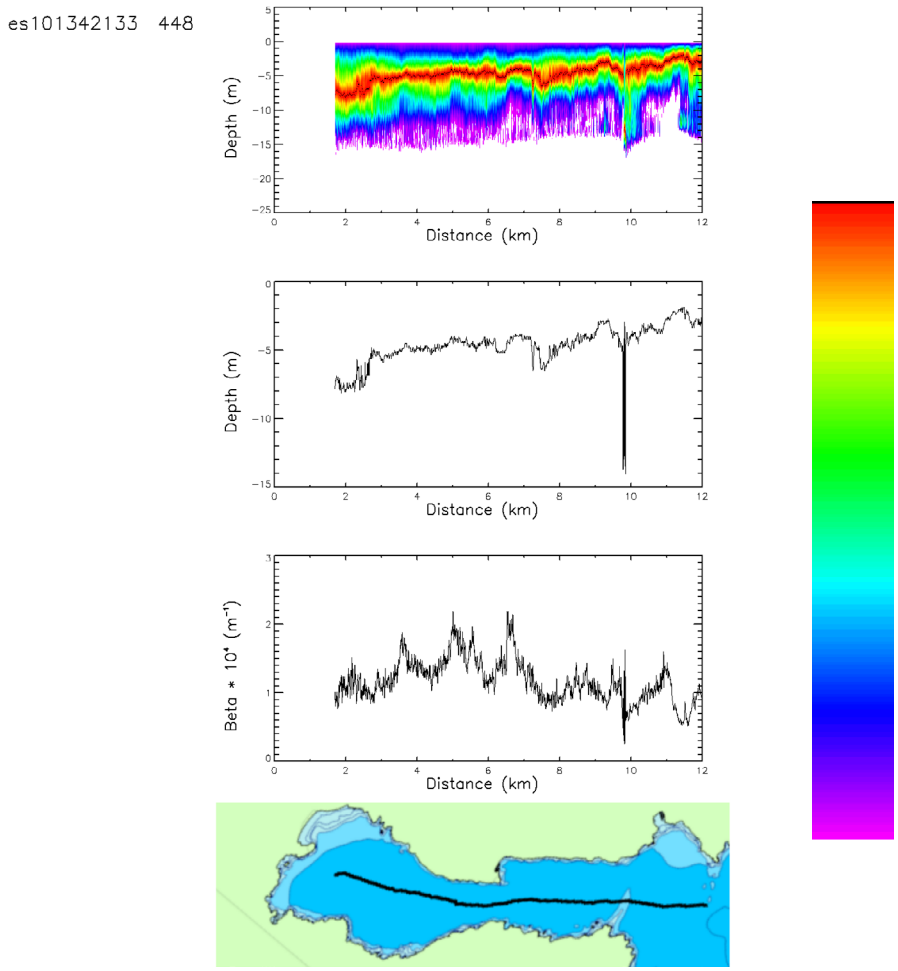

Fig. 3. Stacked plot of a typical lidar transect, plotted as functions of distance from the head of the sound. Top panel is the normalized lidar echogram for the co-polarized channel, plotted using the color bar to the right. Next panel is the depth of the peak return in each lidar pulse. Third panel is the cross-polarized volume scattering coefficient (at a scattering angle of π radians) for the peak returns. Bottom panel is a chart of the sound, rotated to align with the other panels, showing the transect flight track.

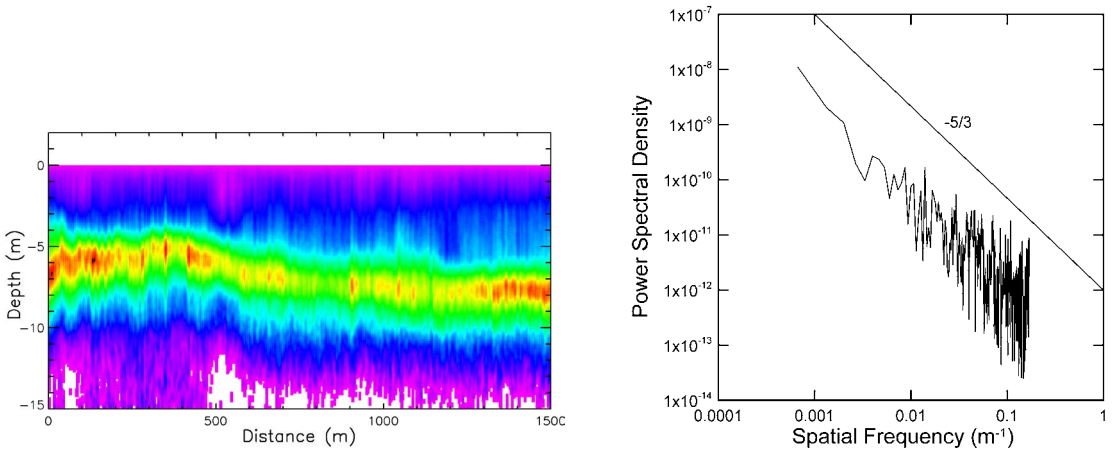

Fig. 4. Echogram of a segment of phytoplankton layer (left) and the power spectral density of the backscattering magnitude at the peak (right). Right panel also shows the -5/3 power law characteristic of a turbulent spectrum.

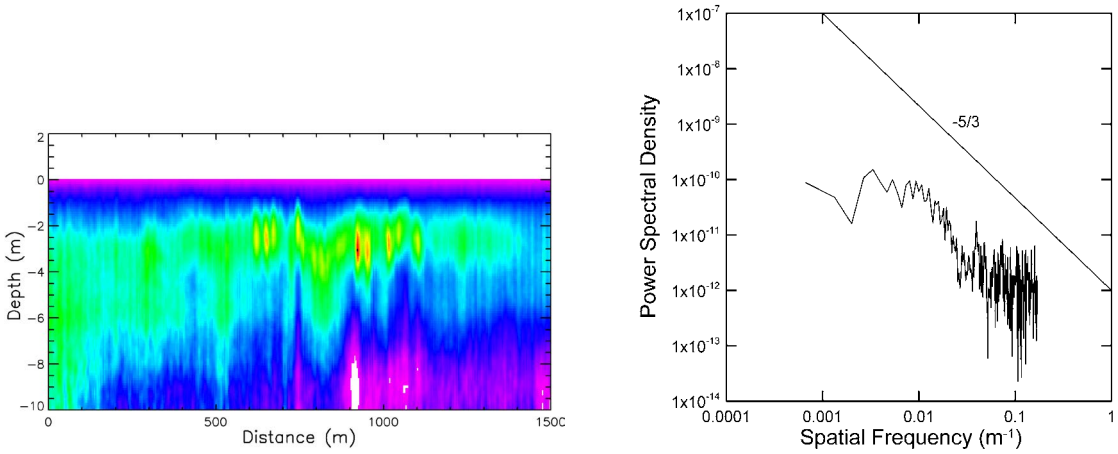

Fig. 5. Echogram of a segment of zooplankton layer (left) and the power spectral density of the backscattering magnitude at the peak (right). Right panel also shows the -5/3 power law characteristic of a turbulent spectrum.

IMPACT/APPLICATIONS

Our re-analysis of 80,000 km of data collected by the NOAA airborne fish lidar developed by Dr. Churnside has shown that this system has the capability to rapidly detect and synoptically sample the spatial extent, intensity and prevalence of thin (and not so thin) backscattering layers in a wide variety of coastal and oceanic waters (Churnside and Donaghay, 2009). The specialized optics, extremely high data rates (10^9 samples/sec), 5 to 10 m horizontal resolution and better than 50 cm vertical resolution of the fish lidar provide an unparalleled synoptic picture of optical fine structure of the upper 50 m of the ocean. Our search for thin layers in this data not only greatly increased our understanding of the

spatial extent and the types of environments where thin layers can occur, but it has also given us new insights into the role of large scale forcing in controlling their occurrence. For example, not only was it shown that thin layers can be equally prevalent in shallow and deep ocean environments during upwelling relaxation events, but also that thin layers can extend uninterrupted for more than 10 km in regions with strong internal wave activity. However, since *in situ* verification/validation efforts have thus far been driven by the need to rapidly assess fish stocks (NOAA's objective in developing the lidar), we can only speculate about the source of the thin layers that are so evident in the data.

In the analyses of the data completed to date, we have shown unequivocally that the layers observed in the lidar return correspond to biological scattering layers through simultaneous in-water measurements of the optical and biological properties of those layers. These data will allow us to develop algorithms that will greatly increase the amount of information that the Navy will be able to infer from current and future lidar systems. Examples from these data include quantitative measurements of internal waves and turbulence levels. We are particularly excited about the potential breakthroughs that will occur when we can combine (a) recent advances in bio-physical modeling, (b) the capabilities of airborne lidar to spatially map fine-scale structure, and (c) the capabilities of autonomous profilers to quantify temporal and spatial changes in fine-scale physical, chemical, bio-optical and bio-acoustical structure.

RELATED PROJECTS

This is a joint project with Drs. Donaghay, Sullivan, and Rines at the University of Rhode Island. The title of their portion is the same, but they are funded through a grant.

REFERENCES

Churnside, J. H. (2008) Polarization effects on oceanographic lidar. Opt. Exp. **16**, 1196-1207.

Churnside, J. H. and P. L. Donaghay (2009) Thin scattering layers observed by airborne lidar. ICES J. Mar. Sci. **66,** 778-789.